An active solar desalination system integrated with collective condenser heat pipe solar evacuated tube collector: a thermoeconomic analysis

Garima Nema[1] · Karunamurthy Krishnasamy[1]

Abstract

An experimental investigation was executed on the solar evacuated tube collector containing a collective condenser unit of heat pipe arrangement attached to a single slope solar desalination system. The brackish water preheating was done by the unique solar collector before entering the still. Performance analysis of the system was carried out with 0.001, 0.002 and 0.003 kg/s brackish water flow rate in the collector and 0.01, 0.02 and 0.03 m of brine water depth in a single-slope solar desalination system. The feasibility of the proposed system was evaluated by thermodynamic analysis, embodied energy, CO_2 mitigation and economic analysis. Active desalination system with collective condenser heat pipe evacuated tube collector at 0.001 kg/s brackish water flow rate and 0.01 m water depth produced maximum freshwater yield, average daily thermal and exergy efficiency of 3.085 l/m²day, 30.25% and 3.17% respectively. An increase of maximum freshwater yield of 37.11% and average daily thermal efficiency of 43.5% respectively were achieved at a brackish water flow rate of 0.001 kg/s and 0.01 m of basin water depth in comparison with a traditional single slope solar desalination system. The embodied energy of the system was estimated as 630.77 kWh, and 0.001 kg/s and 0.01 m of water depth resulted in the highest earned carbon credit of 16,954.48 INR. The minimum payback period of 2.19 years was achieved at the lower brackish water flow rate and basin water depth of 0.001 kg/s and 0.01 m respectively.

Keywords Collective condenser · Heat pipe · Solar desalination · Thermodynamic analysis · Embodied energy · Economic analysis

Nomenclature

A	Area (m²)
AAC	Aggregate annual cost (INR)
ACC	Annual capital cost (INR)
ASV	Annual salvage value (INR)
C_p	Specific heat capacity (J/kg K)
CC	Capital cost (INR)
CF	Cash flow (INR)
CSF	Capital salvage factor
D	Diameter (m)
d	Thickness (m)
E	Energy (kWh)
ECC	Earned Carbon credit
EPF	Energy production factor
EPT	Energy payback time (years)
ET	Evacuated Tube
EX	Exergy
F	Radiation shape factor
g	Acceleration due to gravity (9.81 m/s²)
G	Glass
h	Convective heat transfer coefficient (W/m²K)
HP	Heat pipe
I	Solar radiation intensity (W/m²)
IWT	Inlet water temp. (°C)
k	Thermal conductivity (W/m² K)
LCCE	Life cycle conversion efficiency
L	Latent heat (J/kg)
l	Length (m)
$m°$	Hourly productivity (l/h)
M	Total mass (kg)
m	Mass (kg)

✉ Garima Nema
  garima.nema2018@vitstudent.ac.in

1 School of Mechanical Engineering, Vellore Institute
   of Technology, Chennai 600127, India

n	Life of system (Years)
N	Total number
Np	Payback period
OWT	Outlet water temp.
P	Productivity (l)
Q	Rate of heat transfer (W)
RC	Running cost (INR)
R	Thermal resistance (K/W)
SFF	Sinking fund factor
SP	Selling price (INR)
SV	Salvage value
T	Temperature (°C)
t	Total
U	Uncertainty

Subscripts/Superscripts

a	Air
ab	Absorber
amb	Ambient
b	Basin
C	Collector
c	Condenser
cond	Conduction
conv	Convection
e	Evaporator
en	Entered
evap	Evaporation
i	Inner
in	Input
lq	Liquid
O	Outer glass covers
out	Output
r	Rate of interest
rad	Radiation
ss	Solar still
s	Sky
v	Vapour
w	Water
ws	Wind speed (m/s)
y	Yearly

Greek letters

τ	Transmittance
α	Absorptivity
μ	Dynamic viscosity (Pa s)
η	Efficiency
ρ	Density (kg/m^3)
θ	Angle
σ	Stefan Boltzmann constant (5.67×10^{-8} W/m^2.K^4)
ϵ	Emissivity
π	Pi (3.14)

Introduction

Coastal places of our planet earth have unlimited saline water but limited freshwater sources. The limited fresh water and plenty of saline water areas preferred a desalination process as an auspicious solution to fulfil the demand of inhabitants (Zheng and Hatzell 2020). Desalination of brackish water is an energy-rigorous process. The energy demand is fulfilled by conventional or non-conventional energy sources. Regrettably, conventional energy sources are expensive, diminishing reserves and environmental degradation, leading to developing the interest of researchers to couple desalination systems with non-conventional energy source "solar energy" (Subramanian et al. 2021). Solar energy is one of the most freely available, never exhausting and eco-friendly. Solar energy on the planet earth is utmost suitable for more sunshine continental areas.

The solar thermal desalination process is the topmost assuring adaptive pathway to alleviate worldwide water needs. However, the productivity of solar thermal desalination systems, i.e. solar still, is low. Research, renovations and reviews of regular reform were reported to upsurge the productivity of traditional solar still with different structural designs (Fallahzadeh et al. 2020); variations in productivity-dependent parameters such as additional heating and cooling system for enhancing basin brine water temperature and reducing condensing top cover temperature respectively (Omara et al. 2017; Manish et al. 2020); usage of nanoparticles in various forms such as nanofluids, nano-enriched thermal storage and absorber coatings (Selimefendigil et al. 2022) and sensible (Khechekhouche et al. 2019) and latent heat storage materials (Rashid et al. 2019) integration of different collectors (Yadav 1991). The main objective of the suggested modifications is to increase the water temperature existing in the basin of the desalination system, to improve the distillate yield.

Coupling solar still with collectors is one of the efficient technologies for increasing basin water temperature. Flat plate, parabolic trough and evacuated tube (ET) collectors were used for coupling the solar still. A flat plate collector was integrated by a solar desalination system in natural and forced modes (Yadav 1991). The maximum basin water temperature achieved by the coupled system during the forced mode of circulation was 56 °C. Mathematical modelling was used to compare the efficiency between traditional solar still and collector-coupled solar still in thermosyphon and forced mode of water circulation. Maximum productivity was obtained by the collector-coupled system during the forced mode of water circulation.

Two cases were presented (Akashdeep et al. 2022) for comparing the efficiency at similar atmospheric parameters of a modified desalination system with a traditional

single-slope solar desalination device. This modified system worked with the water flow rate of 0.041 kg/s in the collector. In one case, the arrangement was the combination of a flat plate collector containing a wick which was placed horizontally. However, for the second case, the flat plate collector was integrated with the tilted basin wick solar still at 30°. The reason behind this improvement is the higher temperatures achieved in various components of the system during the second case. The daily efficiency of a modified desalination system was higher by 12.1% in the first case as compared with traditional solar desalination devices, and 16.3% was higher in the second case as compared to case 1 (Akashdeep et al. 2022).

Evacuated tube solar collector gains more attention in the present era for solar thermal applications (Kalogirou 2004). These collectors have high thermal efficiency due to their spherical shape; it does not require a tracking mechanism and the minimum convection and conduction losses between the surrounding and absorbing surface (Mahdjuri 1979). The use of a heat pipe is one of the efficient methods, used to transfer the energy from the evacuated tube to the medium to be heated (Khairnasov and Naumova 2016). He et al. (2012) carried out the experimentation for the generation of electricity and water heating by combining the evacuated tube solar collector containing heat pipe with the thermoelectric generator. The temperature of the water was obtained at 45 °C at the solar intensity of 600 W/m². A comparative study was done to analyse the performance of direct flow and heat pipes containing solar evacuated tube collectors. It shows that the system having a heat pipe gives better performance as compared to the direct flow arrangement (Nkwetta et al. 2013).

Daghigh and Shafieian (2016) perform an energy and exergy analysis in the solar water heating arrangement. It contains evacuated tubes with a heat pipe to analyse the performance parameters. The result represents that the 15 tubes show better performance, and the collector delivers the maximum outlet temperature of the water was 64 °C with maximum exergy of 5.4%. Abo-Elfadl et al. (2020) presented an experimental study for the assessment of energy and exergy analysis by the "integration of reflectors with the evacuated tube solar collector containing heat pipe on its thermal storage". A thermal model was presented and analysed for the selection of reflector positions at different angles. Abi Mathew and Thangavel (2021) use an evacuated tube collector of 20 tubes integrated with the heat pipe for the heating of air at different mass flow rates. Results show that the maximum air temperature of 118 °C was achieved (Abi Mathew and Thangavel 2021).

Some modification was also done by eliminating the solar still from the desalination system. Sadrhosseini (2015) experimented on a 'twin glass evacuated tube' which was used as a collector and basin. Brine water was directly filled into the evacuated tubes. The water absorbs the heat directly from the tubes and starts boiling. The vapours rise and condense in the condensation chamber. The condensed vapour was collected in a jar as freshwater. Distilled water (0.99 l) was produced from this system when tubes were filled with brackish water and under shading (Sadrhosseini 2015). In the same manner, another modification was done by Mosleh et al. (2015) with 65.2% efficiency of the system analysed, while a heat pipe containing an evacuated tube coupled with a parabolic trough collector by a tracking mechanism. Oil and aluminium foil were filled between the heat pipe and the evacuated tube. The filler material is used for system efficiency enhancement by increasing thermal conductivity.

A traditional solar desalination system was coupled with a parabolic trough collector containing an evacuated tube on the focusing axis to receive maximum solar radiation and a serpentine heat exchanger under the basin PCM (Khairat Dawood et al. 2020). Different heat transfer fluid was used in the serpentine heat exchanger at different flow rates for transferring the heat to improve basin water temperature. Variation in water depth (1.5 and 3 cm) was also analysed during the study. The maximum outlet basin water temperature was 78 °C achieved by nano-oil at 0.5 l/min as working fluid at 1.5 cm of basin water depth.

The traditional desalination unit was combined by an evacuated tube collector and rotating hollow cylinder, improving the efficiency by 292% from the traditional single slope solar still. Two modifications were done to improve productivity. The first modification was done inside the still basin where the cylinder drum is rotating to improve the evaporation rate as well as reduce the thickness of the idle basin water layer. Another modification was done to integrate a still by an evacuated tube collector to preheat the basin's brackish water (Alwan et al. 2020).

Another integration of single slope solar still with an evacuated tube solar collector and external condenser section was reported in the literature (Shahin et al. 2022). The use of a heat pipe integrated solar collector was used for improving the basin's saline water temperature, and a wind ventilator was used as an external condenser to decrease the glass cover temperature. The reason behind this arrangement was to increase the temperature difference between saline water and glass cover. Due to the higher temperature difference, more distilled water was obtained from the system. Due to the wind ventilator, the pressure inside the solar still was decreased, and the vapour of the water was moved to the external condenser and condensed on the copper plate of cooling arrangements. This new arrangement of desalination was 2.13 times as compared to the conventional desalination system. This arrangement was also analysed for CO_2 mitigation based on environmental (29.19 tons) and exergo-environmental (0.51 tons) analysis (Shahin et al. 2022).

Kumar et al. (2014) used single-slope solar still which was coupled with 10 evacuated tubes, and a pump is used

for forced circulation. In this arrangement, water was filled inside the evacuated tubes as well as the basin. Bottom basin water was circulated through the pump for enhancing efficiency. In this system, the author developed a theoretical MATLAB program based on experimental data. The maximum energy and exergy efficiencies were obtained at 33.8% and 2.6% at maximum yield (Kumar et al. 2014).

It was analysed from the literature that research was done on the single slope solar still to increase the production of fresh water. Earlier modifications have tried to improve the production capacity by adding PCM, using sensible heating, latent heat storage materials, cooling methods and integration of other supplementary units like PV modules. Due to these modifications previously designed and noted active solar desalination system was costly and less efficient. Previous studies were done on the evacuated tube and heat pipe for water heating and air heating application, but only limited research was done on traditional single-slope solar desalination systems coupled with heat pipe–integrated evacuated twin glass tubes. Earlier developed evacuated tube collectors were directly filled with water, containing an individual heat pipe evaporator and condenser section in each evacuated twin glass tube, and the evacuated tube collector was inserted directly into the solar still basin. Due to the individual condenser unit of each heat pipe, intermittent heating takes place, and the temperature was not increased as per the available energy. In prior studies, the heat pipes were used to carry the heat of evacuated tubes and release it directly inside the basin of the desalination device, and they had separate evaporator, adiabatic and condenser units. Modifications of the solar desalination system without complexity, expensive, space constraint are not dealt by the previous researchers. Most of the studies were done by varying the basin water depth and flow rate of heat transfer fluid, but the present study was done on the evacuated twin glass tube containing heat pipes for different brackish water flow rates and water depths in single slope solar still.

Scope and novelty

This innovative and incomparable approach was exploited to enhance the daily productivity of the traditional solar still. The experimental establishment comprises a combination of two solar units. The first collector unit was used for preheating brackish water by use of an evacuated glass tube containing a sole collective condenser heat pipe unit at different water flow rates, and another unit was used for the evaporation and condensation of freshwater droplets at different basin water depths in single slope solar still.

The novelty of this newly introduced collector in the present procedure embraces evacuated twin glass tubes and a heat pipe arrangement with a distinctively designed working for enhancing the water temperature. The unique

heat pipe contains the sole collective condenser which was connected with the individual evaporator heat pipe units. Due to this novel design, water is heated equally and uniformly from all directions. Since the temperature of brackish water increases rapidly as a feed of solar still, then due to enhanced evaporation, the productivity of the final product as freshwater was boosted. The performance of a new collector system integrated with solar still was designed, fabricated, analysed and tested by thermal and exergy analysis, embodied energy, CO_2 mitigation and economic analysis. The present collector system has evacuated tubes with mild steel heat pipes, so it is cost-effective. This system is small and simple, and it does not require any electric accessories for running, so it is economical. The solar desalination system reported in the recent literature uses ETC with independent condenser heat pipes.

Materials and methods

This section describes the construction and design arrangement of the experimental unit. It also presents the different modified analyses done during experimental studies. Measuring the instrument's accuracy and uncertainty was also performed during the study.

Layout and design of CCHPSETC-SSSD system

Figures 1 and 2 show the experimental and schematic arrangement of a novel collective condenser heat pipe solar evacuated tube collector coupled with a single-slope solar desalination system (CCHPSETC-SSSD). This experimental arrangement comprises two solar units. The first unit of the system was a collective condenser heat pipe solar evacuated tube collector (CCHPSETC) which was used to preheat the brackish water. The second unit of the experimental arrangement was a single slope solar desalination (SSSD) system which was used for the process of evaporation and condensation during the desalination purpose of brackish water. These two systems were connected in series for the continuous and smooth-running flow of brackish water to minimise the temperature from one system to another due to the insulation provided in each unit.

Table 1 represents the detailed specification of the CCHPSETC-SSSD system which absorbs maximum solar energy due to its inclination angle (14°), which was equal to the location latitude.

The CCHPSETC was the first unit of this experimental arrangement of the system. It contains 05 glass evacuated tubes combined with a collective condenser heat pipe and supported on the mild steel frame. The solar evacuated tube collectors were attached to a new heat pipe arrangement called a collective condenser heat pipe. The newly

Fig. 1 Experimental setup of CCHPSETC -SSSD system

Fig. 2 Schematic diagram of experimental analysis rig arrangement
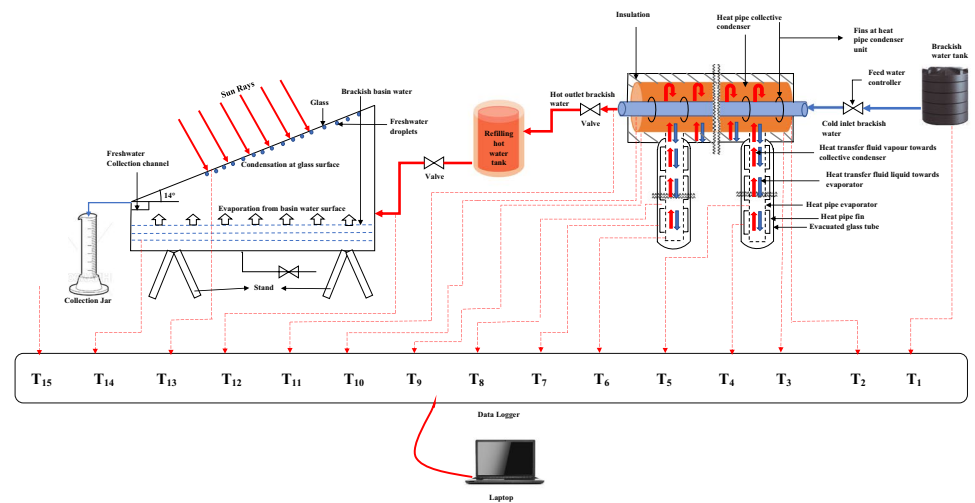
developed collective condenser heat pipe system is responsible for brackish water preheating. Three different mass flow rates were maintained by gravity to reduce the cost of running and maintenance, and it was measured by modular rotameter; the backflow of brackish water was prevented by the non-return valve for analysis of the designed system unit.

The key features of the CCHPSETC introduced during the study that differentiates it from other existing heat pipe–based solar collectors were:

- The heat pipe unit in the present work comprises 05 evaporator units which were placed inside the evacuated tubes. All

05 units of the heat pipe evaporator unit were connected with the one sole heat pipe condenser unit

- The vacuum pressure of 200 mm of mercury was maintained at the entire heat pipe unit, and the saturation temperature was found 91.6 °C

- The header of the solar collector unit was covered with polyurethane foam to minimize the heat rejection from the heat pipe condenser unit. It comprises the condenser unit of the heat pipe and the brackish water flow pipe

- Water was used as a working fluid inside the heat pipe evaporator unit in such a way that during water vapour, condensation equally goes into the evaporator pipe

Table 1 Specification of the CCHPSETC-SSSD system

Elements	Specifications
No. of evacuated glass tubes in the collector	05
Evacuated glass tube length	1800 mm
The outer diameter of an evacuated glass tube	58 mm
The inner diameter of an evacuated glass tube	47 mm
Heat pipe evaporator unit length	1500 mm
The outer diameter of the heat pipe evaporator	12.5 mm
The inner diameter of the heat pipe evaporator	9.3 mm
The thickness of the heat pipe	1.6 mm
No. of fins in one heat pipe	10
The outer diameter of the condenser unit of a heat pipe	75 mm
The inner diameter of the condenser unit of a heat pipe	71 mm
The total length of the condenser unit of the collector	520 mm
Outer Diameter of brackish water pipe	33 mm
Inner Diameter of brackish water pipe	30 mm
Material of heat pipe and brackish water pipe	Mild steel
Fins on the brackish water pipe	4 fins/25 mm
Insulation material for collector header	Polyurethane Foam
The surface area of the solar still basin	1000×1000 mm^2
The material of the solar still	Aluminum
The thickness of the covering glass	4 mm
Glass properties	Scratch resistant
Thermal conductivity of the glass cover	0.78 W/m K
Solar collector and still glass cover angle	14°
Insulation material on solar still	Glass wool
The thickness of insulation for collector and solar still	50 mm

- A water flow pipe was placed inside the condenser unit of the heat pipe so that the heat developed inside the heat pipe will be directly transferred to the water uniformly from all directions
- Fins were connected to the evaporator unit of heat pipes and kept inside the evacuated tubes to increase the heat transfer rate
- Cold water at a constant water flow rate was passed through the brackish water flow pipe present in the condenser unit of a heat pipe. Water gets heated and was ejected from the other side of the water flow pipe

An active SSSD system which was a second unit used for experimentation had a 1-m^2 surface area of the basin. Single-slope solar still was used in this study due to its easy fabrication, simple geometry, being ready to install, economical, skilled labour is not required to operate so rural people can also use it, installation at any geographical location is effective, and less operating and maintenance cost. The bottom basin plate of the SSSD system was painted black due to its absorptivity and the emissivity value is one, with zero reflectivity and transmissivity for all wavelengths. The top covering of the solar desalination system was made up of transparent inclined glass (transmissivity = 0.95) for two reasons. Firstly, maintaining a latitude

angle to absorb maximum solar radiation and the second was to provide a flow of accumulated condensing fresh water vapours for collection of distillate freshwater. Silicon rubber was placed between the top frame of the solar desalination device and the glass cover, to avoid leakage losses of vapour. Window putty was used further to seal the glass cover externally. Three small openings were provided on the SSSD system; one is for the input of preheated brackish water, the second is for the gathering of freshwater droplet output, and the third was for the removal of residual brackish water and maintaining the basin water depth inside the solar still at the basin bottom. A channel was used to collect the distillate water droplets, which accumulated on the glass cover. A feed water tank had been used to supply untreated water inside the collector through the MS pipe with insulation for preheating.

Experimental procedure

The experimental setup consists of a feed water tank, feed valve, CCHPSETC, hot water storage tank, SSSDS, measuring flask, stopwatch, data logger, laptop and thermocouple wires. Before starting to take the readings, the system was running for 24 h for approaching the steady-state condition. Performance analysis was done on the measured parameters such as ambient

temperature, solar radiation intensity, wind speed, inlet and outlet water temperature, raw water flow rate, basin and glass cover temperature and quantity of distilled water. All the readings were measured in 15 min. Temperatures were measured by thermocouple wires, and the temperature was recorded in the laptop through the data logger.

Evacuated tubes of the collector absorbed the solar radiation which was fallen on it. The heat absorbed by the solar collector tubes was transferred through the evaporator wall of the heat pipe to the heat transfer fluid (water). This heat-transferred fluid absorbed the heat and started to evaporate. The evaporated vapour of the heat transfer fluid from all the evaporators of heat pipes reaches the sole collective condenser of the heat pipe. Vapours in the sole collective condenser condense over the water pipe by transferring their heat to brackish water present inside the water pipe. Due to heat, the brackish water gets heated and collected into the hot water tank through an insulated pipe. The desalination unit was filled with preheated water from the hot water tank. Every hour, refilling of hot brackish water was done to maintain the brackish water depth in the basin and enhance the basin water temperature by removing the bottom layer of the cold water from the valve present at the bottom of the solar desalination unit. The desalination unit also absorbs solar radiation through a transparent glass cover. Due to this radiation, the temperature of basin water starts increasing and further vaporises. The vapours were condensing on the glass cover plate due to the temperature differences between the basin and the glass cover. After condensation of these vapours, the freshwater was sliding down on the glass due to its inclination and collected into the distillate pipe. This pipe collected all the fresh water and sends it out from the desalination unit. This freshwater was collected into the measuring flask and measured the quantity every hour for performance analysis.

Instrumentation and uncertainty analysis

The performance of the present study was analysed based on experimental recorded parameters. However, errors and uncertainty were arising from the instruments during selection and calibration, observations and readings. Uncertainty analysis was done to minimise the errors for various experimental recorded parameters such as temperature, solar radiation intensity, wind speed and quantity of water. Overall uncertainty (U_{EXP}) during the measurement of recorded parameters was evaluated from Eqs. 1–6 (Akpinar 2010; Tiwari and Tiwari 2016; Chauhan et al. 2018). Total uncertainty occurred during the measurement of global and diffuse solar radiation (U_{SR}) from solar power meter (SPM) and reading errors (R) is

$$U_{\mathrm{SR}} = \sqrt[2]{U_{\mathrm{SPM}}{}^2 + U_R{}^2} \qquad (1)$$

Total uncertainty occurred during the measurement of temperature (U_T) from thermocouples (TH), a data logger (DL), and reading errors (R) is

$$U_T = \sqrt[2]{U_{TH}^2 + U_{DL}{}^2 + U_R{}^2} \qquad (2)$$

Total uncertainty occurred during the measurement of wind speed (U_{ws}) from anemometer (A) and reading errors (R) is

$$U_{WS} = \sqrt[2]{U_A{}^2 + U_R{}^2} \qquad (3)$$

Total uncertainty occurred during the measurement of productivity (U_P) from the measuring jar (MJ) and reading errors (R) is

$$U_P = \sqrt[2]{U_{MJ}{}^2 + U_R{}^2} \qquad (4)$$

Total uncertainty occurred during the measurement of water flow rate (U_{WFR}) from modular rotameter (MR) and reading error (R) is

$$U_{\mathrm{WFR}} = \sqrt[2]{U_{MR}{}^2 + U_R{}^2} \qquad (5)$$

Overall measured uncertainty during the experimentation was evaluated as:

$$U_{\mathrm{EXP}} = \sqrt[2]{U_{SR}^2 + U_T^2 + U_{WS}^2 + U_P^2 + U_{\mathrm{WFR}}^2} \qquad (6)$$

Table 2 Details of instruments and uncertainties

Parameters	Device	Units	Measuring range	Model	Least count	Uncertainty error (%)
Solar radiation intensity	Solar power meter	W/m^2	0–2000	TENMARS TM207	0.1	0.14
Temperature	Thermocouple	˚C	0–1100	K-Type	0.1	0.17
	Data logger			Masseuses 85 xx		
Wind speed	Anemometer	m/s	0.2–30	Lutron AM-4202	0.1	0.14
Water flow rate	Modular rotameter	ml/min	6–300	SKU-22548	1	1.41
Water quantity	Measuring cylinder flask	ml	0–1000	WKM KT160BI	1	1.41

The calculated experimental uncertainty was found ± 3.27%, which was very low and within the acceptable limit. Table 2 shows the details of instruments and their uncertainties used during experimentation for measuring the various parameters.

Studied cases

The performance of the CCHPSETC-SSSD system was conducted based on fifteen different experimental case studies from set 1 to set 15 by varying the water flow rate and depth of basin water. The flow rate of saline water was varying from 0.001 to 0.003 kg/s and was measured by the modular rotameter. The depth of basin water was also varying from 0.01 to 0.03 m by measuring scale which was kept in the solar still to analyse the performance of the solar. A detailed description of the water flow rate and depth of basin water during each set of an experiment is shown in the Table 3.

The combined performance of the CCHPSETC-SSSD system was analysed from set 1 to set 9. CCHPSETC performance was analysed from set 10 to 12 by varying the water flow rate, and SSSD system performance was analysed from set 13 to 15 by varying basin water depth respectively.

Analysis of the CCHPSETC-SSSD system

Thermodynamic analysis

Thermodynamic analysis of CCHPSETC

The energy and exergy study of the designed CCHPSETC has been carried out in this section, and the following

Table 3 Sets of experimentation

Set number of experimental case studies	CCHPSETC (water flow rate in kg/s)	SSSD (depth of basin water in m)
1	0.001	0.01
2	0.001	0.02
3	0.001	0.03
4	0.002	0.01
5	0.002	0.02
6	0.002	0.03
7	0.003	0.01
8	0.003	0.02
9	0.003	0.03
10	0.001	0
11	0.002	0
12	0.003	0
13	0	0.01
14	0	0.02
15	0	0.03

assumptions were made during the analysis (Shafieian et al. 2019):

- The temperature variation was considered only in the radial direction.
- All equations were applicable for steady-state flow conditions.
- Kinetic and potential energies were assumed negligible.
- There were no chemical or nuclear reactions occurred in the system.
- The specific heat capacity of water is constant.
- The direction of heat transfer towards the system was positive.

Figure 3 shows the solar radiation absorption and heat loss process which is occurred in the solar collector and heat pipe. Evacuated glass tubes absorb a part of sun rays which is incident on it. This heat is absorbed by the heat pipe evaporator unit. The heat transfer fluid is thus evaporated, and vapour is filled in the heat pipe collective condenser unit. The heat was directly transferred from the heat pipe condenser unit to the brackish water and again returns to the evaporator unit, and the cycle continues till solar energy is available on the glass tubes.

Theoretical energy balance is described by the following equations:

Equation 7 shows the solar radiation absorbed in the evacuated glass tube by the spherical surface. The total heat absorbed is the difference between the entire amount of heat energy entering the evacuated glass tube and the amount of heat lost to the atmosphere. (Wang et al. 2012):

$$Q_{ab} = Q_{en} - Q_{loss} \tag{7}$$

where Eq. 8 represents Q_{en} which is the solar radiation entering the evacuated glass tube solar collector, and Q_{loss} is the loss of energy to the atmosphere (Eq. 9) (Azad 2008; Daghigh and Shafieian 2016):

$$Q_{en} = \tau_{GO}\tau_{Gi}\alpha_C A_{ab} N_{ET} I \tag{8}$$

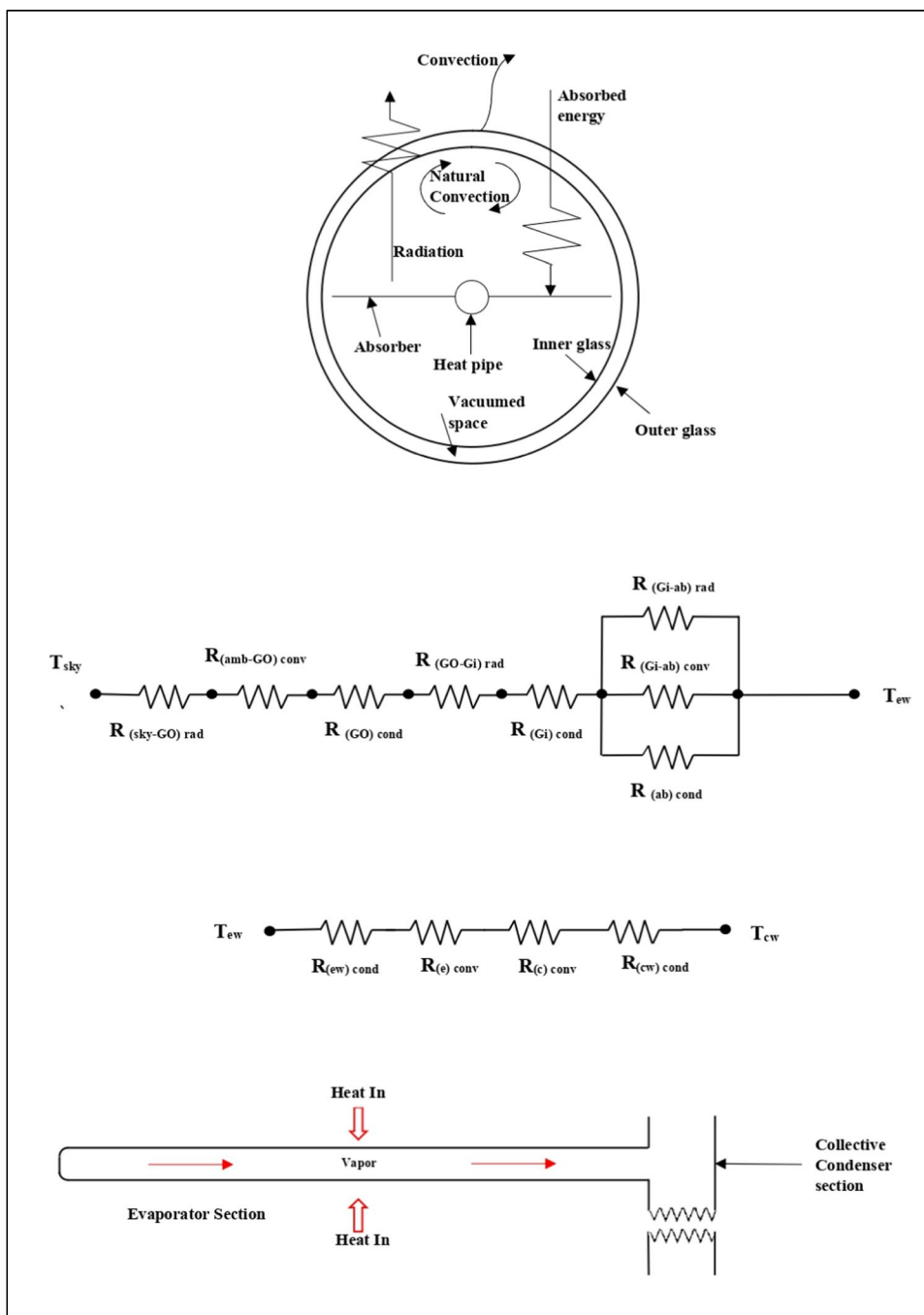$$Q_{loss} = \frac{N_{ET}(T_{ab} - T_{amb})}{R_t} \tag{9}$$

The total thermal resistance (R_t) shown in Fig. 3 is the summation of thermal resistances from the evacuated glass tubes and heat pipe (Azad 2008; Reay et al. 2016):

$$R_t = R_{ET} + R_{HP} \tag{10}$$

where R_{ET} and R_{HP} can be represented by Eqs. 11 and 12, respectively:

Fig. 3 Solar radiation absorption and developed thermal resistance in the CCHPSETC system

$$R_{ET} = R_{(sky-GO)rad} + R_{(amb-GO)conv} + R_{(GO)cond} + R_{(GO-Gi)rad}$$
$$+ R_{(Gi)cond} + R_{(Gi-ab)conv} + R_{(Gi-ab)rad} + R_{(ab)cond} \tag{11}$$

$$R_{HP} = R_{(ew)cond} + R_{(e)conv} + R_{(c)conv} + R_{(cw)cond} \tag{12}$$

The sky is assumed as a black body so emissivity is assumed as one (Hlaing and Soe 2014):

$$R_{(sky-GO)rad} = \frac{1}{A_{GO}\sigma(T_{GO} + T_{sky})(T_{GO}^2 + T_{sky}^2)} \tag{13}$$

Sky temperature can be calculated by Eq. 14:

$$T_{sky} = 0.0552 \times T_{amb}^{1.5} \tag{14}$$

Convective resistance between the outer evacuated glass tube and the ambient is determined by (Chopra et al. 2019)

$$R_{(Go-amb)conv} = \frac{1}{h_{amb}.A_{GO}} \qquad (15)$$

Conduction thermal resistance due to the outer glass tube can be represented (Chopra et al. 2019):

$$R_{(Go)cond} = \frac{ln(\frac{D_{GO,o}}{D_{GO,i}})}{2\pi K_G l_G} \qquad (16)$$

The radiation thermal resistance is present between the outer and inner glass tube (Daghigh and Shafieian 2016):

$$R_{(Gi-GO)rad} = \frac{\frac{1-\epsilon_{Gi}}{\epsilon_{Gi} A_{Gi}} + \frac{1}{A_{Gi}F_{Gi-GO}} + \frac{1-\epsilon_{GO}}{\epsilon_{GO}A_{GO}}}{\sigma(T_{Gi} + T_{GO})(T_{Gi}^2 + T_{GO}^2)} \qquad (17)$$

The thermal resistance due to conduction for the inner glass tube is calculated as

$$R_{(Gi)cond} = \frac{ln(\frac{D_{Gi,O}}{D_{Gi,i}})}{2\pi K_G l_G} \qquad (18)$$

Convection thermal resistance between the absorber and inner glass tube can be represented (Chopra et al. 2019):

$$R_{(ab-Gi)conv} = \frac{1}{h_a(\frac{A_{ab}+A_{Gi}}{2})} \qquad (19)$$

The radiation thermal resistance between the absorber and inner glass tube is given by (Reay et al. 2016; Chopra et al. 2019)

$$R_{(ab-Gi)rad} = \frac{\frac{1-\epsilon_{ab}}{\epsilon_{ab} A_{ab}} + \frac{1}{A_{ab}F_{ab-G}} + \frac{1-\epsilon_{Gi}}{\epsilon_{Gi}A_{Gi}}}{\sigma(T_{ab} + T_{Gi})(T_{ab}^2 + T_{Gi}^2)} \qquad (20)$$

A conduction thermal loss between the absorber and inner borosilicate glass tube can be represented as (Cengel 2007)

$$R_{(ab-Gi)cond} = \frac{d_{ab}}{K_{ab}.A_{ab}} \qquad (21)$$

Conduction thermal resistance due to the evaporator wall and condenser wall can be calculated (Azad 2008; Daghigh and Shafieian 2016)

$$R_{(e,w)cond.} = \frac{ln\left(\frac{D_{e,o}}{D_{e,i}}\right)}{2\pi K_{(e,w)} l_e} \qquad (22)$$

$$R_{(c,w)cond.} = \frac{ln\left(\frac{D_{c,o}}{D_{c,i}}\right)}{2\pi K_{(c,w)}.l_c} \qquad (23)$$

The thermal resistance due to the flow of heat transfer fluid in the evaporator and condenser unit of the heat pipe during the process of evaporation and condensation is given as (Azad 2008; Daghigh and Shafieian 2016)

$$R_{(e,i)conv.} = \frac{1}{h_e\pi D_{(e,i)}l_e} \qquad (24)$$

$$h_e = \frac{K_e}{t_e} \qquad (25)$$

$$R_{(c,i)conv} = \frac{1}{h_c\pi D_{(c,i)}l_c} \qquad (26)$$

$$h_c = 0.728\left[\frac{g\,sin\,\theta\rho_{lq}(\rho_{lq} - \rho_v)K^3 h_{fg}}{D\mu_{Iq}\Delta T_{lq}}\right] \qquad (27)$$

Thermodynamic energy efficiency was calculated as the ratio of total heat absorbed by the brackish water to the total heat absorbed by the collector. The heat absorbed by the brackish water and CCHPSETC efficiency can be calculated by Eqs. 28 and 29 respectively (Cengel 2007):

$$Q_{abs} = m_w\left[c_{p,w}\left(T_{w,O} - T_{w,i}\right)\right] \qquad (28)$$

$$\eta = \frac{m_w[C_{p,w}(T_{w,O} - T_{w,i})]}{IA_C} \qquad (29)$$

The thermodynamic exergy analysis was performed to represent the energy quality of the system, based on the second law of thermodynamics by figuring out and comprehending the reasons for the system's inefficiencies. It helps to design an energy-efficient system by identifying the parameters, which results in the thermodynamic imperfections of the system. The thermodynamic exergy efficiency can be defined as the ratio of valuable delivered exergy (EX_V) to absorb exergy by the collector (EX_C) (Gunerhan and Hepbasli 2007):

$$\eta_{EX} = \frac{EX_V}{EX_C} \qquad (30)$$

where valuable delivered exergy and absorbed exergy by the collector were calculated by Eqs. 31 and 32 respectively (Petela 2003) (Abi Mathew and Thangavel 2021)

$$EX_V = m_w^{\circ} C_{p,w}[(T_{amb} - T_{w,i}) - T_{amb}\left(ln\frac{T_O}{T_{w,i}}\right)] \qquad (31)$$

$$EX_C = A_C I\left[1 + \left\{\left(\frac{1}{3}\right)\left(\frac{T_{amb}}{T_s}\right)^4\right\} - \left\{\left(\frac{4}{3}\right)\left(ln\frac{T_{amb}}{T_s}\right)\right\}\right] \qquad (32)$$

T_s is the solar radiation temperature which is 6000 K (Petela 2003).

Thermodynamic analysis of the SSSD system

The SSSD system was used in the proposed system for the evaporation and condensation of basin water. The thermodynamic thermal and exergy analysis of the SSSD system was calculated by the heat balance equations with the following assumptions (Kumar et al. 2014; Agrawal and Rana 2018):

- Heat capacity and thermal resistive losses of the glass cover plate were neglected.
- The glass cover plate inclination was small.
- Vapour leakage losses from the solar still were assumed as negligible.
- Losses from the side walls and the bottom wall were assumed as negligible.
- A steady-state regime was assumed for the heat transfer process during system operation on an experimental day.
- Constant depth of basin water was assumed in the SSSD system.

The hourly productivity m° of fresh water by the SSSD system was given as (Sampathkumar et al. 2010; Rahbar and Esfahani 2013)

$$m° = \frac{Q_{evap}}{h_{fg}} \times 3600 \times A_{ss} \tag{33}$$

where evaporative heat transfer (Q_{evap}) occurs between basin water and the inner glass cover and was evaluated as (Sampathkumar et al. 2010)

$$Q_{evap} = h_{evap}(T_{bw} - T_{Gi}) \tag{34}$$

Dunkle's semi-empirical relation was used to evaluate the evaporative (h_e) and convective (h_c) heat transfer coefficients from Eqs. 35 and 36 (Sampathkumar et al. 2010):

$$h_e = 0.016273 \times h_c \times \frac{P_{bw} - P_{Gi}}{T_{bw} - T_{Gi}} \tag{35}$$

$$h_c = 0.884 \left[(T_{bw} - T_{Gi}) + \frac{(P_{bw} - P_{Gi})(T_{bw} + 273)}{(268.9 \times 10^3 - P_{bw})} \right]^{1/3} \tag{36}$$

Partial vapour pressure at basin water and inner glass was evaluated by Eqs. 37 and 38 (Rahbar and Esfahani 2013):

$$P_{bw} = \exp\left(25.317 - \frac{5144}{T_{bw} + 273}\right) \tag{37}$$

$$P_{Gi} = \exp\left(25.317 - \frac{5144}{T_{Gi} + 273}\right) \tag{38}$$

The daily thermal efficiency of the SSSD system was evaluated by Eq. 39 (Elbar and Hassan 2020):

$$\eta = \frac{M_{ew} \times L}{\sum I(t) \times A_b \times 3600} \tag{39}$$

where M_{ew} was the total daily mass of water evaporated by the SSSD system.

The exergy efficiency of the solar still can be defined as the ratio of exergy output associated with the product (i.e. distillate yield) to the exergy input (radiation exergy) and can be expressed as (Kumar and Tiwari 2011):

$$\eta_{EX} = \frac{\text{Output exergy of SSS Dsystem } (EX_o)}{\text{Input exergy of SSS Dsystem } (EX_i)}$$

where EX_O and EX_i were calculated by Eqs. 40 and 41 respectively (Kumar and Tiwari 2011):

$$EX_O = h_e \times A_b (T_{bw} - T_{Gi}) \left(1 - \frac{T_a}{T_{bW}}\right) \tag{40}$$

$$EX_i = A_G \times I(t) \times \left[1 - \frac{4}{3} \times \left(\frac{T_{amb}}{T_s}\right) + \frac{1}{3} \times \left(\frac{T_{amb}}{T_s}\right)^4\right] \tag{41}$$

Energy analysis

Energy matrix

Energy analysis is one of the critical parameters due to the hike in fuel charges, crude material supply, and effect on nature. This section comprises the energy analysis of the developed CCHPSETC-SSSD system which consists of embodied energy, energy payback time, energy production factor, life cycle conversion efficiency and thermal efficiency. Embodied energy is defined as the total energy involved in the system fabrication of a unit. The energy consumption level of the system is indicated by the embodied energy. The process of measuring embodied energy comprises the total essential energy to take out the raw material, material transportation and distribution to the site, production and maintenance of parts and elements associated with the designed system. The energy consumption level contributes to greenhouse gases and is responsible for environmental degradation (Shrivastava and Kumar 2017).

The energy matrix of the CCHPSETC-SSSD system was calculated from Eqs. 42–44 (Kumar 2013). Energy payback time (EPT) is calculated by the ratio of invested embodied

energy during the manufacturing of the system to the annual production of energy by the system (Kumar et al. 2020):

$$EPT = \frac{E_{in}}{E_{out}} \tag{42}$$

The energy production factor (EPF) is evaluated as the ratio of the lifetime production of the energy by the system to the invested embodied energy during the manufacturing of the system. It is also defined as the inverse of the energy payback time and used to predict the total system performance (Kumar 2013):

$$EPF = \frac{E_{out}}{E_{in}} \times n \tag{43}$$

Life cycle conversion efficiency (LCCE) is defined as the ratio of the net energy productivity of the system to the lifetime solar energy input for the system (E_{in}). The numeric value of LCCE is always less than one. If it is nearer to one then that technology will be the best from the energy point of view (Singh et al. 2018):

$$LCCE = \frac{E_{out} \times n - E_{in}}{E_{in,s} \times n} \times 100 \tag{44}$$

Enviro-economic analysis

This section discusses the emission of greenhouse gases, CO_2 mitigation and earned carbon credits. Indian coal-based power plant generates 1 kWh of electricity by emitting 0.98, 0.008 and 0.003 kg of CO_2, SO_2 and NO respectively. In India, the transmission and distribution losses are considered as 40% and 20%; hence, emissions of CO_2, SO_2 and NO are considered as 1.58, 0.012 and 0.005 kg respectively (Kumar 2013; Singh and Samsher 2020):

$$\text{Lifetime emission of } CO_2 = E_{in} \times 1.58 \tag{45}$$

CO_2 emission and mitigation are crucial parameters to evaluate the potential of climatic change. It refers to the net quantity of CO_2 that has been saved throughout life in terms of kg of CO_2 mitigation. It is calculated from Eq. 46 (Singh and Samsher 2020):

$$\text{Net lifetime } CO_2 \text{ mitigation (kg)} = (E_{out} \times n - E_{in}) \times 1.58 \tag{46}$$

The saleable net quantity of CO_2 mitigation is referred to as carbon credit. It is sold out for profit in terms of economic value. Carbon credits which are traded in the energy market are referred to as earned carbon credit (ECC). Each ECC is equivalent to a tonne of CO_2 and saleable at the fluctuating price of 5 to \$20/tonne of CO_2 mitigation (Kumar et al. 2020):

$$ECC = \text{Net lifetime } CO_2 \text{ mitigation (tonnes)} \times C \tag{47}$$

where C is the saleable price of ECC in the energy market and assumed as US\$9.99 per tonne of CO_2 (Singh and Samsher 2020) (US\$9.99 = 79.65 INR dated 20 Sept 2022).

Economic analysis

The financial viability of the CCHPSETC-SSSD system was determined based on the per unit cost of desalination and the payback period. The unit cost of desalination depends on the parameters such as capital cost (CC), the annual rate of interest (r), the life of the desalination unit (n), salvage value (SV), yearly productivity (MDW_{yearly}) and yearly operation and maintenance cost (Ranjan et al. 2016).

The unit cost for desalination of brackish water (DW_{uc}) is calculated as (Sharon and Reddy 2015)

$$DW_{uc} = \frac{AAC(\text{Aggregate Annual Cost})}{MDW_{yearly}} \tag{48}$$

The aggregate annual cost of the CCHPSETC-SSSD system is determined (Rajaseenivasan and Srithar 2016):

$$AAC = ACC + RC - ASV \tag{49}$$

where RC is running cost

$$\text{Annual capital cost (ACC)} = CC \times CSF \tag{50}$$

where Capital Salvage Factor (CSF) was calculated by (Rajaseenivasan and Srithar 2016)

$$CSF = \frac{r(1 + r)^n}{(1 + r)^n - 1} \tag{51}$$

Annual salvage value (ASV) was determined by the product of salvage value (SV) and sinking fund factor (SFF) (Rajaseenivasan and Srithar 2016)

$$ASV = SV \times SFF \tag{52}$$

where

$$SFF = \frac{r}{[(1 + r)^n - 1]} \tag{53}$$

The average yearly mass of distilled water produced can be evaluated by the product of average daily distilled water productivity (m_d) of the CCHPSETC-SSSD system and the overall number of bright days in a year (N_d) as:

$$MDW_y = m_d \times N_d \tag{54}$$

The payback period (N_p) of the CCHPSETC-SSSD system is calculated as (Sharon and Reddy 2015)

$$N_p = \frac{ln\left[\frac{CF}{CF-(CC\times r)}\right]}{ln[1+r]} \tag{55}$$

Cash flow (CF) can be calculated as the product of the selling price (S_p) sold in the market and the produced quantity of distilled water from the desalination system (Ranjan et al. 2016):
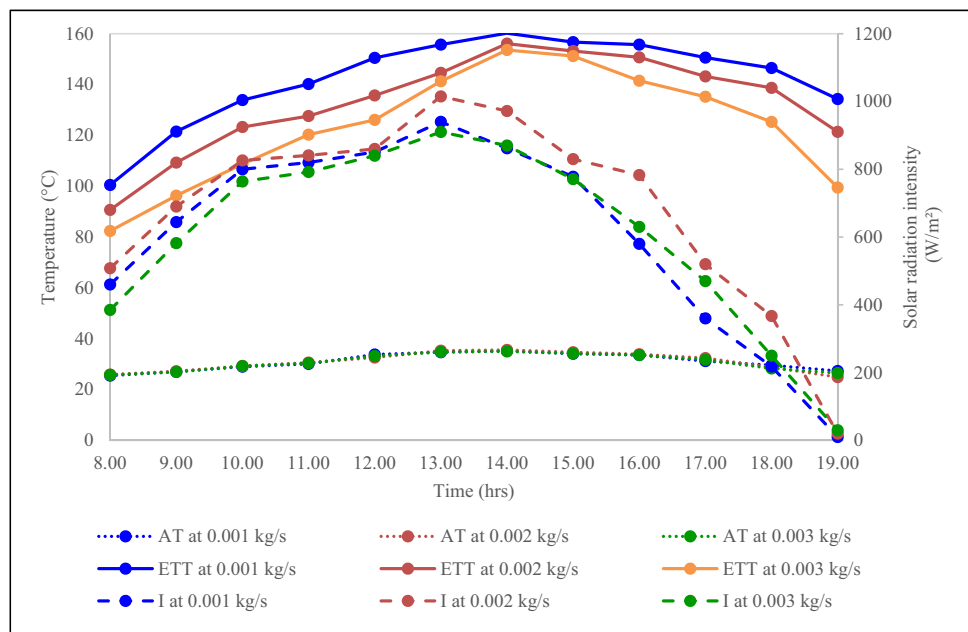
$$CF = MDW_y \times S_p \tag{56}$$

Results and discussion

The CCHPSETC-SSSD system studies were carried out experimentally, and readings were noted from 8.00 to 19.00 h in Chennai, India, from April to July 2020. During the experimentation, solar radiation intensity, brackish water flow rate, basin water depth, the quantity of distilled water and all the temperatures including ambient, evacuated tube, heat pipe evaporator and condenser, inlet and outlet water temperature, basin water and glass cover temperatures were noted for the combination of all the three water mass flow rates and basin water depths. To analyse the various parameters for evaluating the collector performance, 0.001, 0.002 and 0.003 kg/s inlet water flow rates were used. The performance study of the desalination system was also carried out with and without a collector at various basin water depths of 0.01, 0.02 and 0.03 m respectively.

Variation of ambient temperature, solar radiation and evacuated tube temperature

Figure 4 represents the average variation of solar radiation intensity (I), ambient (AT) and evacuated tube temperature

(ETT) with time. Maximum solar radiation and ambient temperature during all the experimental sets were recorded at 13.00 h and 14.00 h respectively. During the experiment, the average ambient temperature, solar radiation intensity and evacuated tube temperature were recorded between 29.8 and 32.1 °C, 605 and 684 W/m² and 123.45 and 142.19 °C respectively. Experimental value reveals that a higher value of solar radiation and ambient temperature increased the productivity of the CCHPSETC-SSSD system. It was also noted that the temperature inside the evacuated tube was reduced when the mass flow rate was increased. The same pattern of ambient temperature and solar radiation with time was attained and also revealed that the higher value of solar radiation and ambient temperature can enhance productivity (Mevada et al. 2021). It was seen that the temperature inside the evacuated tube was retained even after sunset, and the maximum evacuated tube temperature was varying from 156.1 to 153.6 °C for water flow rates ranging from 0.001 to 0.003 kg/s. The heat was present inside the evacuated tube during off-sunshine hours because the evacuated tube was perfectly fitted and insulated at the header unit of the collector. Abi Mathew and Thangavel (2021) reported the maximum evacuated tube temperature of 154 °C during the variation of airflow rate in an evacuated tube solar dryer (Abi Mathew and Thangavel 2021).

Variation of heat pipe temperatures with time

Figure 5 represents the experimental observation of the solar collector in which the heat pipe evaporator and condenser temperature (HPET and HPCT) increases from morning and attains a maximum value between 14.00 and

Fig. 4 Variation of ambient temperature, solar radiation and evacuated tube temperature with time

Fig. 5 Variation of heat pipe temperatures with time
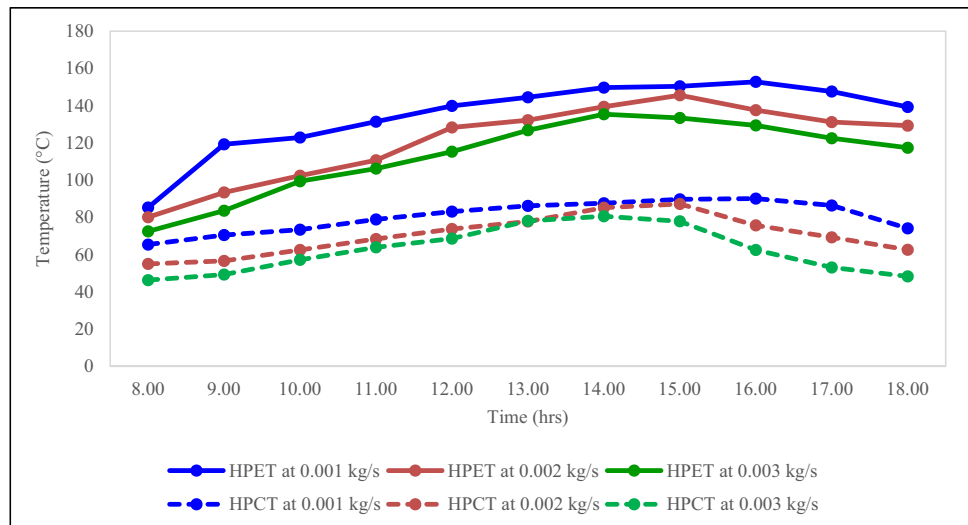
16.00 h. All the temperatures of the evaporator and condenser unit were recorded with the help of thermocouple wires attached to the data logger. The experimental observations show that the rate of heat transfer increases significantly from the evacuated glass tube to the heat pipe evaporator from 8.00 h due to the increased solar radiation intensity. The heat pipe evaporator exhibits higher temperatures of 152.8 °C at 16.10 h for 0.001 kg/s of water flow rate. Similarly, the maximum temperature of the heat pipe evaporator for 0.002 kg/s and 0.003 kg/s was 145.6 °C and 135.4 °C at 15.15 h and 13.50 h respectively.

The heat was flowing from the heat pipe evaporator to the collective condenser unit with the help of heat transfer fluid. The maximum temperature of the heat pipe collective condenser recorded was 90.1 °C for 0.001 kg/s water flow rate at 16.10 h. Similarly, the maximum condenser temperature achieved for 0.002 kg/s and 0.003 kg/s was 87.2 °C and 80.6 °C at 15.15 h and 13.50 h respectively. The variation

in time to achieve maximum temperature was due to the stored heat in the collector unit and the water flow rate. Thus, a high amount of heat was retained inside the evacuated tube for a longer time when the lower water flow rate of 0.001 kg/s was maintained.
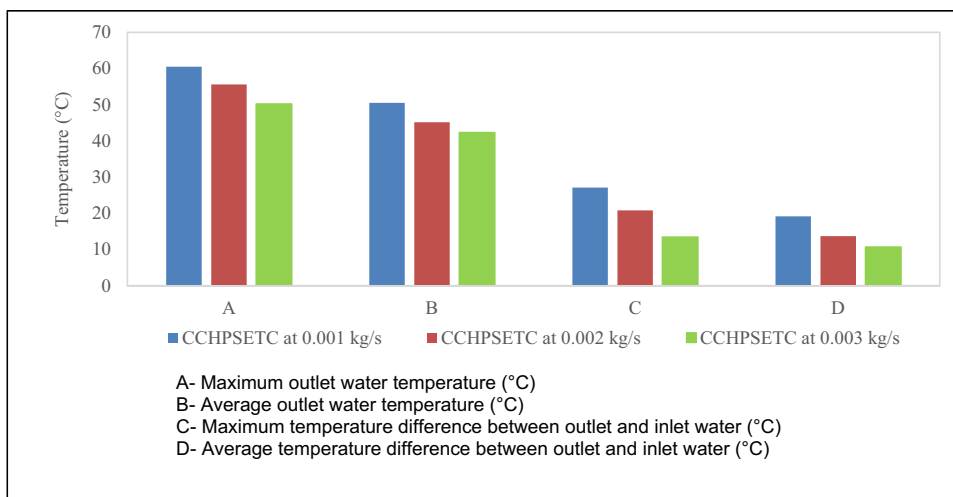
Inlet and outlet water temperature with time and water flow rate

Figure 6 depicts the collector's hourly inlet and outlet water temperature (IWT and OWT) during 0.001 to 0.003 kg/s water flow rate. It was observed that the collector outlet water temperature mainly depends on the water flow rate. The maximum outlet water temperature from the collector was 60.5 °C, 55.6 °C and 50.2 °C during 0.001, 0.002 and 0.003 kg/s at 16.10 h, 15.15 h and 13.50 h respectively. The maximum temperature difference between outlet and inlet water was noted as 27.1 °C during

Fig. 6 Variation of inlet and outlet water temperatures with time for varying water flow rates
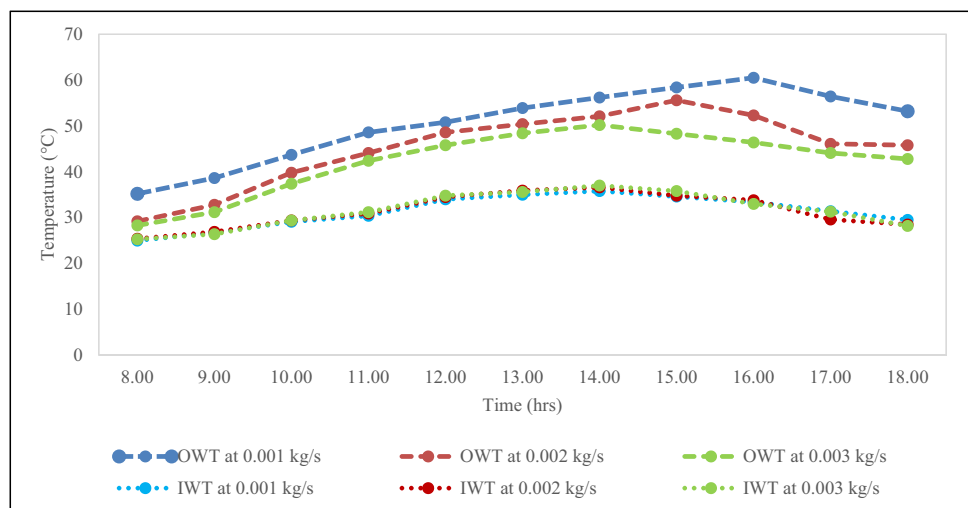
Fig. 7 Temperature of CCHPSETC water at a different water flow rate

A- Maximum outlet water temperature (°C)
B- Average outlet water temperature (°C)
C- Maximum temperature difference between outlet and inlet water (°C)
D- Average temperature difference between outlet and inlet water (°C)

the water flow rate of 0.001 kg/s. The decreasing trend of temperature difference was observed between the outlet and inlet water for a water flow rate of 0.001 to 0.003 kg/s. During a low water flow rate of 0.001 kg/s, inlet water gets enough time to take out the heat from the collective condenser heat pipe and attained a higher outlet water temperature. Figure 7 depicts the maximum and average outlet water temperature and the difference between outlet and inlet water temperatures.

Variation of basin water temperature, glass cover temperature with water flow rate and basin water depth

Figures 8 and 9 represent the hourly values for the temperature of basin water and glass cover respectively for

CCHPSETC-SSSDS and traditional SSSD systems. The temperature of basin water and glass cover attained the highest values at 14.00 h for CSDS which were 69, 65.04, 63 °C and 60, 53.81, 52 °C with the depth of basin water varying from 0.01,0.02, 0.03 m respectively. Whereas for the CCHPSETC-SSSD system at 0.001 kg/s water flow rate and 0.01 m water depth, the highest values of basin water and glass cover temperature were attained at 16.00 h which was 83.7 °C and 78.91 °C respectively. It was also noted that the temperature of the glass cover was lesser than the basin water temperature. This is due to the glass cover having heat transfer with the surrounding environment. The maximum temperature of basin water and glass cover was observed to be declining with the rise in the depth of basin water from 0.01 to 0.03 m. Results revealed that the time to achieve a maximum of basin

Fig. 8 Basin water temperatures in the CCHPSETC-SSSD system and traditional SSSD system
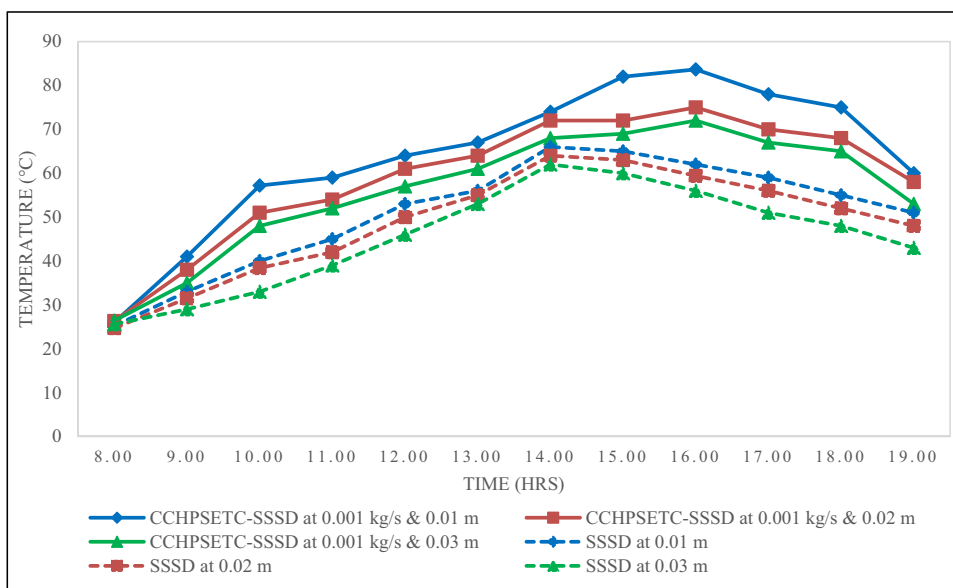
Fig. 9 Glass cover temperatures in CCHPSETC-SSSD system and traditional SSSD system
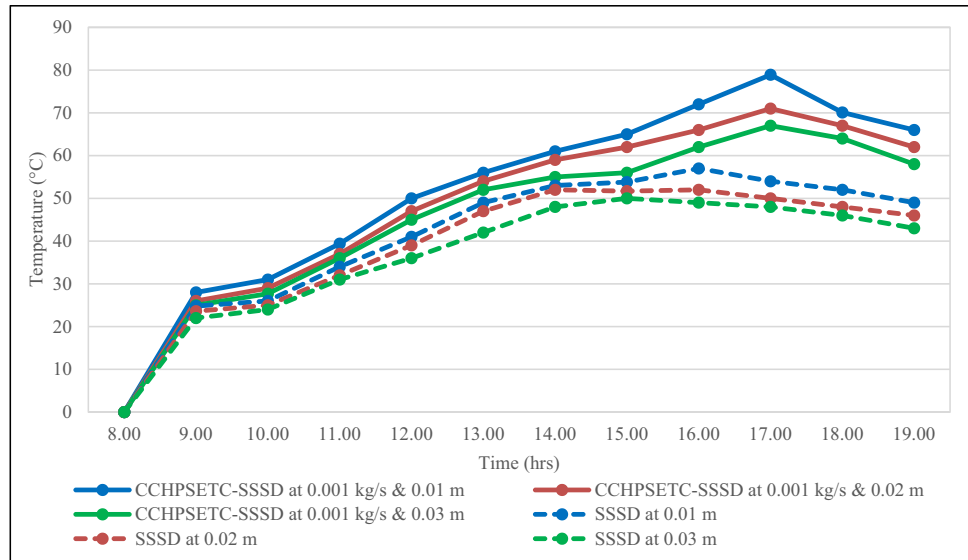
Table 4 Basin water and glass cover temperatures for CCHPSETC-SSSD system at various water flow rates and basin water depth

Water flow rate (kg/s)	Water depth (m)	Basin water temperature (°C)	Glass cover temperature (°C)
0.001	0.01	83.7	78.91
	0.02	75	71
	0.03	72	67
0.002	0.01	60.35	53.47
	0.02	55.31	48.77
	0.03	52.45	46.53
0.003	0.01	54.36	47.58
	0.02	51.59	45.55
	0.03	48.01	42.90

water and glass cover declined from 16.00 to 14.00 h, while the water flow rate increased by 0.001 to 0.003 kg/s respectively. The filled water quantity present inside the collector works as the heat reservoir, and the evacuated

tube solar collector retains the heat into the heat pipe and increases the temperature of basin water till 16.00 h. Continuous and steady heating of water through the heat pipe condenser unit as well as the minimized losses through the collector due to the insulation provided on the manifold were accountable for achieving maximum temperature even after the declination of solar radiation. The temperature of basin water and glass cover increases with an increase in solar radiation (Panchal et al. 2020). A similar trend in variation of basin water temperature and glass cover temperature was observed during the experimental analysis with water flow rates of 0.002 and 0.003 kg/s. The maximum and average values of basin water and glass cover temperature obtained during the study with 0.002 and 0.003 kg/s are as shown in Table 4.

From Table 4, it was observed that the increment in water flow rate and depth reduces the brackish basin water and inner glass temperatures. Alwan et al. (2020) also reported the maximum basin water temperature of 64.2 °C at 14.00 h; however, the maximum solar radiation was 1022 W/m^2 at 13.00 h (Alwan et al. 2020).

Fig. 10 Productivity of CCHPSETC-SSSDS and traditional SSSD system
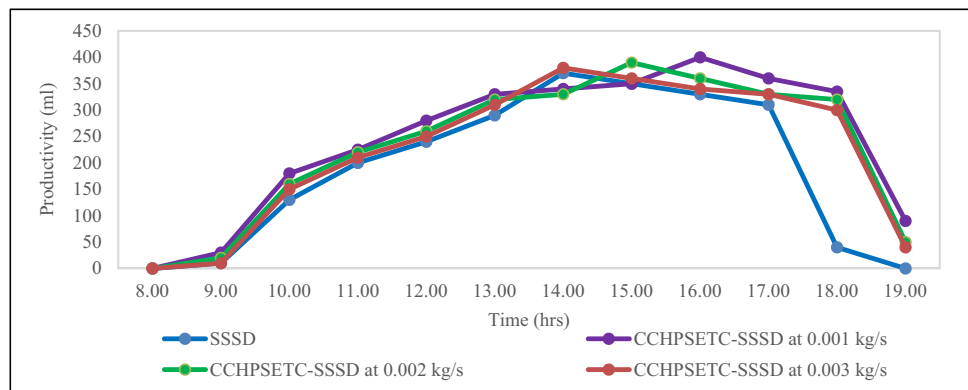
Productivity

The variation of the hourly yield of freshwater with the SSSD system and CCHPSETC-SSSD system with 0.001 kg/s and three depths of water is shown in Fig. 10. The maximum hourly yield of freshwater was obtained for the CCHPSETC-SSSD system with a water flow rate of 0.001 kg/s and brine water depth in the basin of 0.01 m at 16.00 h and which was 0.41 l. Daily collective freshwater yield in the SSSD system and CCHPSETC-SSSD with 0.001 kg/s was observed to decrease from 2.25 to 1.73 l/m^2 and from 3.08 to 2.14 l/m^2 respectively, while a rise in water depth from 0.01 to 0.03 m. Table 5 shows the daily productivity and the maximum hourly freshwater yield for different experimental sets of water flow rate and basin water depth. The highest amount of water evaporation occurs when the depth of water was less due to the less time to attain equilibrium with the surroundings and the use of maximum absorption of solar radiation from the absorber plate. It was also noted that in the SSSD system, the maximum hourly yield was achieved at 14.00 h whereas in the CCHPSETC-SSSD system, as the mass flow rate was increased from 0.001 to 0.003 kg/s at the same water depth, the time to achieve maximum hourly yield was declined to 14.00 h from 16.00 h This variation of time in attaining the maximum hourly yield was mainly due to the combination of preheating of brackish water, storage effect of water heat inside the collector, time interval between vaporization and condensation, the temperature difference between brackish water present in the still basin and glass cover plate, removal of cold water from the basin and recovering the same level with the preheated hot water. This justifies the purpose of integrating the CCHPSETC with the SSSD system to raise the basin water temperature.

Table 6 represents a comparison study of the maximum temperature of basin water, inner glass cover and productivity of the present CCHPSETC-SSSD system with other types of desalination devices developed by the various authors.

The result shows that the present system is delivering higher basin water and inner glass cover temperatures with higher productivity of 3.08 l.

Thermodynamic analysis

This section represents the thermal resistance, heat transfer coefficients and thermal and exergy efficiencies of the CCHPSETC and SSSD systems.

Thermal resistance values obtained from the evacuated tubes were 31.35, 31.99 and 32.76 K/W and by heat pipe were 2.61, 2.93 and 3.15 K/W in the designed CCHPSETC for a water flow rate of 0.001, 0.002 and 0.003 kg/s respectively. Values of thermal resistance show that the variation was insignificant during the variation of water flow rate in the water pipe from 0.001 to 0.003 kg/s. This minimal thermal resistance shows a higher coefficient of heat transfer from the heat pipe evaporator unit to the water pipe.

Table 5 Cumulative daily and maximum hourly productivity at various water flow rates and basin water depth

Water flow rate (kg/s)	Water depth (m)	Cumulative daily productivity (l)	Maximum hourly productivity (l)
0.001	0.02	2.6	0.380
0.002	0.02	2.43	0.375
0.003	0.02	2.305	0.350
–	0.02	2.03	0.350
0.001	0.03	2.14	0.320
0.002	0.03	2.12	0.340
0.003	0.03	1.88	0.320
-	0.03	1.73	0.310

Table 6 Performance comparison study

Type of still	Maximum temperature (°C)		Water depth in the basin (m)	Productivity (l/m^2)	Author (year)
	Basin water	Glass cover			
CCHPSETC-SSSD system	83.66	78.91	0.01	3.08	Present study
	75	71	0.02	2.6	
	72	67	0.03	2.145	
Flat plate collector integrated with modified pyramid solar still	–	–	–	3.0	Subramanian et al. (2021)
Modified pyramid solar still	–	–	–	2.20	
Solar still with inclined fin	69	66	0.01	2.375	Panchal et al. (2020)
Solar still with fin	66	64	0.01	2.32	
evacuated tube collector integrated with a traditional desalination device	83	78	0.01	2.57	Kumar et al. (2014)
	68	65	0.03	1.2	

Table 7 Heat transfer coefficient at different water flow rates and basin water depth

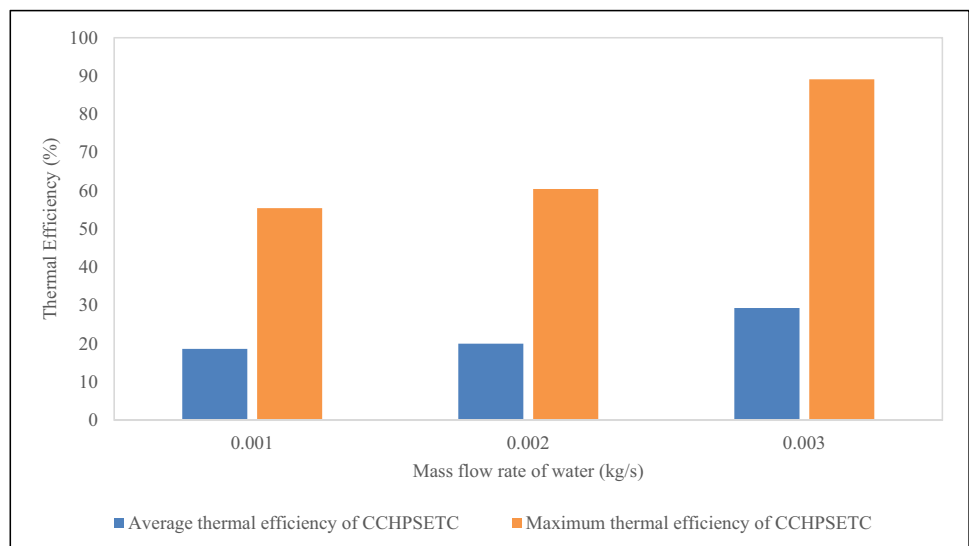| Water flow rate (kg/s)	Water depth (m)	Average heat transfer condensation coefficient h_c (W/m^{2}K)	Average heat transfer evaporation coefficient h_e (W/m^{2}K)	Maximum heat transfer condensation coefficient h_c (W/m^{2}K)	Maximum heat transfer evaporation coefficient h_e (W/m^{2}K)
0.001	0.01	2.33	34.08	2.97	84.19
	0.02	2.12	26.36	2.82	50.54
	0.03	1.96	21.72	2.62	46.08
0.002	0.01	2.14	27.81	3.26	84.81
	0.02	2.02	21.47	2.70	43.43
	0.03	1.92	18.28	2.63	37.48
0.003	0.01	2.03	20.61	2.58	51.26
	0.02	1.92	17.56	2.44	43.86
	0.03	1.78	14.18	2.27	32.81

The values of the maximum and average heat transfer coefficient for evaporation and condensation of the SSSD system are represented in Table 7. The maximum value of the heat transfer coefficient of evaporation and condensation was noted at 16.00, 15.00 and 14.00 h during the water flow rate of 0.001, 0.002 and 0.003 kg/s respectively. The maximum value of the heat transfer coefficient was due to the maximum value of basin water and glass cover temperature at 16.00, 15.00 and 14.00 h for various water flow rates of 0.001, 0.002 and 0.003 kg/s respectively.

The thermal and exergy efficiency of the CCHPSETC for various water flow rates is depicted in Figs. 11 and 12 respectively. It was analysed from the study that higher thermal efficiency of the CCHPSETC was achieved during a higher water flow rate of 0.003 kg/s. It was also noted that the time was inadequate for the water present inside the collector water pipe to absorb heat from the heat pipe condenser unit during the higher water flow rate. This justifies the enhancement of average thermal efficiency of 19%, 20% and 29% and exergy
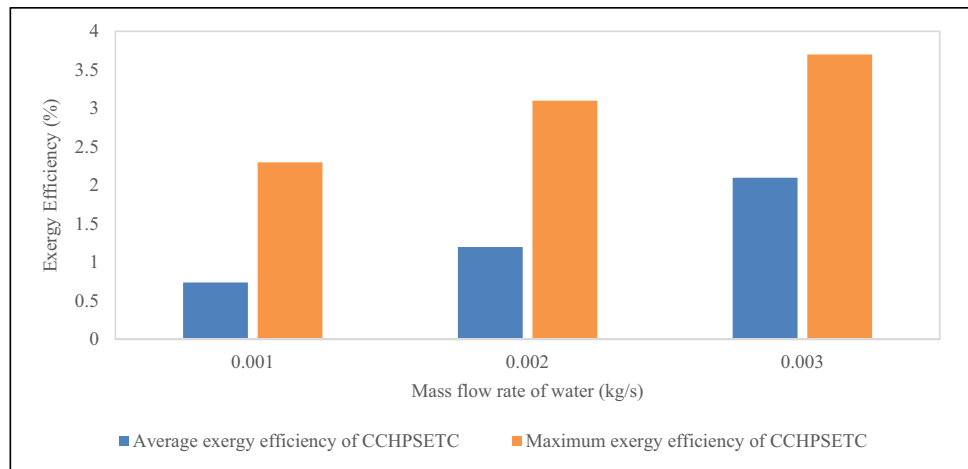
efficiency of 1.54, 1.62 and 1.74% during 0.001, 0.002 and 0.003 kg/s mass flow rates of water respectively. The average thermal efficiency was greater than the exergy efficiency because of the demolition of exergy in the system and the rejection of exergy to the environment.

The thermodynamic efficiency of the traditional SSSD system was also calculated to compare the improvement in the combined CCHPSETC-SSSD system. The thermal and exergy efficiency of traditional solar desalination devices without integration of the CCHPSETC system at a water depth of 0.01, 0.02 and 0.03 m was found at 21.08, 19.11, 15.94% and 1.41, 1.16, 0.81% respectively.

Table 8 shows the daily thermal efficiencies of the combined CCHPSETC-SSSD system for various water depths and different water flow rates. It was observed that the higher thermodynamic efficiency of 30.25% was attained at a lower water depth of 0.01 m and a low water flow rate of 0.001 kg/s. This is due to the higher temperature of outlet water from the collector at a lower water flow rate and higher evaporative heat

Fig. 11 Thermal efficiency at different water flow rates

Fig. 12 Exergy efficiency at different water flow rates

Energy and earned carbon credit analysis of CCHPSETC-SSSD system

Table 9 represents the details of embodied energy associated with each component of the CCHPSETC-SSSD system which was used during manufacturing and maintenance (Kumar et al. 2020; Shoeibi et al. 2021).

Table 10 shows the different energy matrix parameters for all three mass flow rates and water depths, i.e. 0.001, 0.002 and 0.003 kg/s and 0.01, 0.02 and 0.03 m respectively. It was also observed that the total embodied energy of 630.775 kWh was considered for the designed CCHPSETC-SSSD system, and CO_2 emission over a lifetime was evaluated as 0.9966 tons. Both the parameters were independent of mass flow rate and depth of water.

Analysis shows that the minimum energy payback time, maximum payback factor and maximum life cycle conversion efficiency were 1.18 year, 0.85 and 10.6% at 0.001 kg/s water flow rate and 0.01-m water depth. Net annual CO_2 mitigation of 24.26 tons and earned carbon credit of 16,954.48 INR were calculated at 0.001 kg/s water flow rate and 0.01 m

Table 8 Thermodynamic efficiencies of the CCHPSETC-SSSD system

Water flow rate (kg/s)	Water depth (m)	Thermal efficiency (%)	Exergy efficiency (%)
0.001	0.01	30.25	3.17
	0.02	25.77	2.32
	0.03	21.36	1.75
0.002	0.01	26.03	2.46
	0.02	22.61	1.81
	0.03	19.82	1.44
0.003	0.01	24.89	1.91
	0.02	21.60	1.49
	0.03	17.84	1.04

transfer coefficient at lower water depth. It was also noted that the thermal efficiencies of the CCHPSETC-SSSD system were higher than the exergy efficiencies due to the low quality of the output energy.

Table 9 Embodied energy associated with components of CCHPSETC-SSSD system and specifications (Kumar et al. 2020; Singh and Samsher 2020)

Name of component	Material of components	Quantity (kg)	Embodied energy (kWh/kg)	Total (kWh)
Cover plate	Glass	3	11.25	33.75
Sticking solution	Araldite	1	24.1	24.1
Basin liner	Paint	0.5	27.25	13.625
Solar still body	Aluminum	6	55.2	331.2
Water Pipe, Heat pipe, fin and clamp	Mild Steel	5	9.5	47.5
Insulation	Glass wool	4	4.05	16.2
Stand	Iron	4	6.25	25
Evacuated Glass Tubes	Glass	10	11.25	112.5
Raw Water tank and freshwater jar	Plastic	1	23.61	23.61
Gasket	Rubber	1	3.29	3.29

Table 10 Energy matrix parameters of the CCHPSETC-SSSD system

Water flow rate (kg/s)	Depth of basin water (m)	Yearly average Freshwater quantity (l)	Annual Energy output E_{Out} (kWh)	Energy Payback time EPT (years)	Energy Payback factor (EPF)	Lifetime conversion efficiency (LCCE) (%)	Annual CO_2 mitigation over a lifetime (tons)	Annual Earned carbon credit (INR)
0	0.01	619	388.59	1.62	0.62	7.6	17.42	12,172.75
	0.02	558	350.30	1.80	0.56	6.8	15.6	10,904.56
	0.03	476	298.82	2.10	0.48	5.7	13.16	9199.77
0.001	0.01	849	532.98	1.18	0.85	10.6	24.26	16,954.48
	0.02	715	448.86	1.41	0.72	8.8	20.27	14,168.6
	0.03	591	371.01	1.70	0.58	7.2	16.58	11,590.63
0.002	0.01	777	487.78	1.29	0.78	9.6	22.12	15,457.59
	0.02	668	419.35	1.50	0.67	8.2	18.87	13,191.47
	0.03	583	365.99	1.72	0.58	7.15	16.34	11,424.31
0.003	0.01	737	462.67	1.36	0.73	9.1	20.93	14,625.98
	0.02	634	398.01	1.58	0.63	7.8	17.86	12,484.61
	0.03	517	324.56	1.94	0.51	6.2	14.38	10,052.17

Table 11 Parameters for economic analysis

Parameters	Values
Capital cost (INR)	16,000
Annualized capital cost (INR)	1697.268
Running and maintenance cost @ 10% (INR)	236.7541
I @10%	0.1
SV @20%	339.45
Bright days in one year (N)	275
Annualized salvage cost	2.063

water depth. The minimum energy payback time was calculated as 1.3 years while the coupling of solar still with the parabolic trough collector (Kumar et al. 2020).

Economic analysis of the CCHPSETC-SSSD system

Economic analysis of the CCHPSETC-SSSD system was analysed based on an established procedure by Kumar et al. (2020). The present system worked for the period of 11 h/day for 275 bright days in a year. CCHPSETC-SSSD delivered 849–517 kg/year of freshwater by varying the water flow rate from 0.001 to 0.003 kg/s and water depth in the basin from 0.01 to 0.02 m respectively. A complete economic analysis was done for the system based on different parameters shown in Table 11 (Singh and Samsher 2020).

The cost of the freshwater delivered by the CCHPSETC-SSSD system was 2.09 INR/kg, and the system can produce 849 kg/year of fresh water at a flow rate of 0.001 kg/s and 0.01 m brine water depth in the basin. The payback period of 2.19 years was achieved for the designed system while 10 INR is considered the

selling price for 1 l of fresh water in the market. The total quantity of freshwater produced by the system during the life span (*n*) of 30 years will be 24,172.5 kg. Table 12 represents the payback period of the CCHPSETC-SSSD system at different experimental sets during various water flow rates and basin water depths. Commercialization and installation of the system at a high solar radiation location can reduce the payback period and cost of freshwater production. Kumar et al. (2014) found the payback period of 3.7 years due to that the less price of selling water was 6 INR for 1 l of fresh water. The achieved cost of freshwater of is 2.01 INR/kg due to the use of 10 evacuated glass tubes. (Kumar et al. 2014).

Conclusion

The performance of the system with different modifications was compared in the present research work. During experimentation, various parameters such as brackish (saline) water flow rate, inlet water temperature, evacuated tube temperature, heat pipe evaporator and collective condenser temperature, basin water depth and temperature, inner glass cover temperature, solar radiation, ambient temperature and wind speed were measured. The comparisons between the different experimental sets were done on those days when the variations of meteorological parameters remain the same. The following conclusions are drawn from the study of the developed CCHPSETC-SSSD system based on thermodynamic modelling, uncertainty, energy and economic analysis:

- A combination of collective condenser units of the heat pipe and evacuated tube collector in the present system

Table 12 Payback period of CCHPSETC-SSSD system at different experimental sets

Water flow rate (kg/s)	Basin water depth (m)	Annual quantity of distilled water (l)	The unit cost of distilled water (INR)	Payback period (years)
0.00	0.01	619	2.87	3.14
	0.02	558	3.19	3.54
	0.03	476	3.74	4.30
0.001	0.01	849	2.09	2.19
	0.02	715	2.49	2.66
	0.03	591	3.01	3.3
0.002	0.01	777	2.29	2.42
	0.02	668	2.66	2.87
	0.03	583	3.05	3.33
0.003	0.01	737	2.41	2.56
	0.02	634	2.80	3.05
	0.03	517	3.44	3.88

maintains uniform and even heating to obtain the hot outlet brackish water temperature even during less or fluctuating sunshine hours.

- The temperature distribution throughout the heat pipe unit of the system and the temperature of the preheated hot water were greatly influenced by the brackish water flow rate. The maximum collective condenser temperature of the heat pipe unit was achieved at 98.7 °C at 0.001 kg/s and 16.10 h. As the water flow rate increases, the heat pipe temperature and time are reduced and reach 13.00 h
- Average ambient temperature and solar radiation were varying during experimentation from 29.8–32.1 °C and 605–684 W/m^2 respectively. The productivity of the system was directly proportional to the ambient temperature and solar radiation
- The maximum preheated brackish water temperature was 60.5 °C, 55.6 °C and 50.2 °C at a flow rate of 0.001 kg/s, 0.002 kg/s and 0.003 kg/s at 16.10 h, 15.15 h and 13.50 h respectively from the CCHPSETC
- The highest value of basin brackish water temperature was 83.7 °C and the glass cover temperature was 78.91 °C at 0.001 kg/s brackish water flow rate and 0.01 m water depth at 16.00 h in this novel system
- The maximum daily collected freshwater yield was 2.25 l/m^2 in the SSSD system and 3.08 l/m^2 in the novel CCHPSETC-SSSD (0.001 kg/s) at 0.01 m basin water depth in both systems
- The total thermal resistances obtained from novel CCHPSETC were 33.96 K/W, 34.92 K/W and 35.91 K/W at brackish water flow rates of 0.001 kg/s, 0.002 kg/s and 0.003 kg/s respectively
- The thermodynamic thermal efficiencies at 0.01 m, 0.02 m and 0.03 m basin water depth for SSSD were found to be 21.08%, 19.11% and 15.94% while for the novel

CCHPSETC-SSSD system (0.001 kg/s of water flow rate) were found to be 30.25%, 25.77% and 21.36% respectively
- The thermodynamic exergy efficiencies at 0.01 m, 0.02 m and 0.03 m basin water depth for SSSD were found to be 1.41%, 1.16% and 0.81% while for the novel CCHPSETC-SSSD system (0.001 kg/s of water flow rate) were found to be 3.17%, 2.32% and 1.75% respectively.
- The energy matrix of the novel CCHPSETC-SSSD system was calculated at 0.001 kg/s water flow rate and 0.01 m basin water depth. Embodied energy associated with the various components was obtained at 630.775 kWh. The annual energy output was 532.98 kWh, energy payback time 1.18 years, life cycle conversion efficiency 10.6%, CO_2 mitigation 24.26 tons and earned carbon credits 16,954.48 INR.
- The economic analysis represents for the novel system at 0.001 kg/s of brackish water flow rate, and 0.01-m basin water depth can produce 849 l/year of freshwater at the unit cost of 2.09 INR and a payback period of 27 months.

As the above determination establishes at a lower water flow rate of 0.001 kg/s and water depth of 0.01 m, a combination of heat pipe, system temperature distribution, use of maximum preheated brackish water temperature, the highest value of basin water–glass cover temperature, satisfactory daily collected freshwater yield, system thermal resistance, thermal efficiency, exergy efficiency, energy matrix is also markable and the productivity and economic analysis of the system; all are result oriented and encouraging to the success of this system. Finally, it is concluded that the novel CCHPSETC-SSSD system works effectively and efficiently as compared to the SSSD system. This new system is also considered energy-economical-environmental-friendly and best-suitable for littoral locations.

Author contribution Both authors contributed to the concept, design and development of the present work. In addition, this work was carried out as a part of the Ph.D. dissertation of Garima Nema who was supervised by Karunamurthy Krishnasamy. Garima Nema performed the experimental and numerical analyses, collected and interpreted the data and drafted the majority of the manuscript. Krishnasamy Karunamurthy supervised and revised all the data interpretations, analyses and a manuscript.

Data availability Not applicable.

Declarations

Ethical approval This article does not contain any studies with human participants or animals performed by the author.

Consent to participate Not applicable.

Consent for publication This manuscript is an original work produced by the authors. Both (Garima Nema and Karunamurthy Krishnasamy) authors are aware of its content and approve its submission. It is also important to mention that the manuscript has not been published elsewhere in part or entirety and is not under consideration by another journal. We further certify that proper citations to the previously reported work have been given, and no data/table/figures have been quoted verbatim from other publications. The author has given consent for this article to be submitted for publication in Environmental Science and Pollution Research.

Competing interests The authors declare no competing interests.

References

Abi Mathew A, Thangavel V (2021) A novel thermal storage integrated evacuated tube heat pipe solar air heater: energy, exergy, economic and environmental impact analysis. Sol Energy 220:828–842. https://doi.org/10.1016/j.solener.2021.03.057

Abo-Elfadl S, Hassan H, El-Dosoky MF (2020) Energy and exergy assessment of integrating reflectors on thermal energy storage of evacuated tube solar collector-heat pipe system. Sol Energy 209:470–484. https://doi.org/10.1016/j.solener.2020.09.009

Agrawal A, Rana RS (2018) Energy and exergy analysis of single slope single basin solar still in Indian condition: an experimental analysis. Mater Today Proc 5:19656–19666. https://doi.org/10.1016/j.matpr.2018.06.328

Akashdeep N, Gurpinder Singh D, Satbir Singh S (2022) Experimental investigation on single basin tilted wick solar still integrated with flat plate collector. Mater Today Proc 48:1439–1446

Akpinar EK (2010) Drying of mint leaves in a solar dryer and under open sun: modelling, performance analyses. Energy Convers Manag 51:2407–2418. https://doi.org/10.1016/j.enconman.2010.05.005

Alwan NT, Shcheklein SE, Ali OM (2020) Experimental investigation of modified solar still integrated with solar collector. Case Stud Therm Eng 19:100614. https://doi.org/10.1016/j.csite.2020.100614

Azad E (2008) Theoretical and experimental investigation of heat pipe solar collector. Exp Therm Fluid Sci 32:1666–1672. https://doi.org/10.1016/j.expthermflusci.2008.05.011

Cengel YA (2007) Heat transfer-a practical approach, 3rd edn. McGraw-Hill

Chauhan PS, Kumar A, Nuntadusit C (2018) Thermo-environomical and drying kinetics of bitter gourd flakes drying under north wall insulated greenhouse dryer. Sol Energy 162:205–216. https://doi.org/10.1016/j.solener.2018.01.023

Chopra K, Tyagi VV, Pathak AK et al (2019) Experimental performance evaluation of a novel designed phase change material integrated manifold heat pipe evacuated tube solar collector system. Energy Convers Manag 198:111896. https://doi.org/10.1016/j.enconman.2019.111896

Daghigh R, Shafieian A (2016) Theoretical and experimental analysis of thermal performance of a solar water heating system with evacuated tube heat pipe collector. Appl Therm Eng 103:1219–1227. https://doi.org/10.1016/j.applthermaleng.2016.05.034

Elbar ARA, Hassan H (2020) Enhancement of hybrid solar desalination system composed of solar panel and solar still by using porous material and saline water preheating. Sol Energy 204:382–394. https://doi.org/10.1016/j.solener.2020.04.058

Fallahzadeh R, Aref L, Gholamiarjenaki N et al (2020) Experimental investigation of the effect of using water and ethanol as working fluid on the performance of pyramid-shaped solar still integrated with heat pipe solar collector. Sol Energy 207:10–21. https://doi.org/10.1016/j.solener.2020.06.032

Gunerhan H, Hepbasli A (2007) Exergetic modeling and performance evaluation of solar water heating systems for building applications. Energy Build 39:509–516. https://doi.org/10.1016/j.enbuild.2006.09.003

He W, Su Y, Wang YQ et al (2012) A study on incorporation of thermoelectric modules with evacuated-tube heat-pipe solar collectors. Renew Energy 37:142–149. https://doi.org/10.1016/j.renene.2011.06.002

Hlaing S, Soe MM (2014) Design calculation and heat transfer analysis of heat pipe evacuated tube solar collector for water heating. International Journal of Scientific Engineering and Technology Research 3(12):2606–26111. http://ijsetr.com/uploads/321456IJSETR1276-445.pdf

Kalogirou SA (2004) Solar thermal collectors and applications. Prog Energy Combust Sci 30:231–295. https://doi.org/10.1016/j.pecs.2004.02.001

Khairat Dawood MM, Nabil T, Kabeel AE et al (2020) Experimental study of productivity progress for a solar still integrated with parabolic trough collectors with a phase change material in the receiver evacuated tubes and in the still. J Energy Storage 32:102007. https://doi.org/10.1016/j.est.2020.102007

Khairnasov SM, Naumova AM (2016) Heat pipes application to solar energy systems. Appl Sol Energy (english Transl Geliotekhnika) 52:47–60. https://doi.org/10.3103/S0003701X16010060

Khechekhouche A, Haoua BB, Kabeel AE, et al (2019) Improvement of solar distiller productivity by a black metallic plate of zinc as a thermal storage material. J Test Eval 49. https://doi.org/10.1520/JTE20190119

Kumar S (2013) Thermal-economic analysis of a hybrid photovoltaic thermal (PVT) active solar distillation system: role of carbon credit. Urban Clim 5:112–124. https://doi.org/10.1016/j.uclim.2013.07.001

Kumar S, Tiwari GN (2011) Analytical expression for instantaneous exergy efficiency of a shallow basin passive solar still. Int J Therm Sci 50:2543–2549. https://doi.org/10.1016/j.ijthermalsci.2011.06.015

Kumar S, Dubey A, Tiwari GN (2014) A solar still augmented with an evacuated tube collector in forced mode. Desalination 347:15–24. https://doi.org/10.1016/j.desal.2014.05.019

Kumar A, Vyas S, Nchelatebe Nkwetta D (2020) Experimental study of single slope solar still coupled with parabolic trough collector. Mater Sci Energy Technol 3:700–708. https://doi.org/10.1016/j.mset.2020.07.005

Mahdjuri F (1979) Evacuated heat pipe solar collector. Energy Convers 19:85–90. https://doi.org/10.1016/0013-7480(79)90004-4

Manish S, Ashok Kumar S, Singh P (2020) Impact of materials and economic analysis of single slope single basin passive solar still: a review. Mater Today Proc 21:1643–1652. https://doi.org/10.1016/j.matpr.2019.11.289

Mevada D, Panchal H, Sadasivuni KK (2021) Investigation on evacuated tubes coupled solar still with condenser and fins: experimental, exergo-economic and exergo-environment analysis. Case Stud Therm Eng 27:101217. https://doi.org/10.1016/j.csite.2021.101217

Mosleh HJ, Mamouri SJ, Shafii MB, Sima AH (2015) A new desalination system using a combination of heat pipe, evacuated tube and parabolic trough collector. Energy Convers Manag 99:141–150

Nkwetta DN, Smyth M, Haghighat F et al (2013) Experimental performance evaluation and comparative analyses of heat pipe and direct flow augmented solar collectors. Appl Therm Eng 60:225–233. https://doi.org/10.1016/j.applthermaleng.2013.06.059

Omara ZM, Abdullah AS, Kabeel AE, Essa FA (2017) The cooling techniques of the solar stills' glass covers – a review. Renew Sustain Energy Rev 78:176–193. https://doi.org/10.1016/j.rser.2017.04.085

Panchal H, Mevada D, Sadasivuni KK et al (2020) Experimental and water quality analysis of solar stills with vertical and inclined fins. Groundw Sustain Dev 11:100410. https://doi.org/10.1016/j.gsd.2020.100410

Petela R (2003) Exergy of undiluted thermal radiation. Sol Energy 74:469–488. https://doi.org/10.1016/S0038-092X(03)00226-3

Rahbar N, Esfahani JA (2013) Productivity estimation of a single-slope solar still: theoretical and numerical analysis. Energy 49:289–297. https://doi.org/10.1016/j.energy.2012.10.023

Rajaseenivasan T, Srithar K (2016) Performance investigation on solar still with circular and square fins in basin with CO2 mitigation and economic analysis. Desalination 380:66–74. https://doi.org/10.1016/j.desal.2015.11.025

Ranjan KR, Kaushik SC, Panwar NL (2016) Energy and exergy analysis of passive solar distillation systems. Int J Low-Carbon Technol 11:211–221. https://doi.org/10.1093/ijlct/ctt069

Rashid FL, Shareef AS, HFA (2019) Enhancement of fresh water production in solar still using new phase change materials. J Adv Res Fluid Mech Therm Sci 61:63–72

Reay D, McGlen R, Kew P, Dunn PD (2016) Heat pipes. Elsevier Science, Germany

Shahmohamadi M, Shafii MB, Sadrhosseini H (2015) Solar water distillation by using water in the inner glass evacuated tubes. Paper presented in conference named as- 3rd Southern African Solar Energy Conference, South Africa, pp 11–13. http://hdl.handle.net/2263/49481

Sampathkumar K, Arjunan TV, Pitchandi P, Senthilkumar P (2010) Active solar distillation-a detailed review. Renew Sustain Energy Rev 14:1503–1526. https://doi.org/10.1016/j.rser.2010.01.023

Selimefendigil F, Şirin C, Öztop HF (2022) Experimental analysis of combined utilization of CuO nanoparticles in latent heat storage unit and absorber coating in a single-slope solar desalination system. Sol Energy 233:278–286. https://doi.org/10.1016/j.solener.2022.01.039

Shafieian A, Khiadani M, Nosrati A (2019) Thermal performance of an evacuated tube heat pipe solar water heating system in cold season. Appl Therm Eng 149:644–657. https://doi.org/10.1016/j.applthermaleng.2018.12.078

Sharon H, Reddy KS (2015) Performance investigation and enviro-economic analysis of active vertical solar distillation units. Energy 84:794–807. https://doi.org/10.1016/j.energy.2015.03.045

Shoeibi S, Rahbar N, Esfahlani AA, Kargarsharifabad H (2021) Energy matrices, exergoeconomic and enviroeconomic analysis of air-cooled and water-cooled solar still: experimental investigation and numerical simulation. Renew Energy 171:227–244. https://doi.org/10.1016/j.renene.2021.02.081

Shahin S, Hadi K, Nader R, Gholamreza K, Mohsen S (2022) An integrated solar desalination with evacuated tube heat pipe solar collector and new wind ventilator external condenser. Sustain Energy Technol Assessments. https://doi.org/10.1016/j.seta.2021.101857

Shrivastava V, Kumar A (2017) Embodied energy analysis of the indirect solar drying unit. Int J Ambient Energy 38:280–285. https://doi.org/10.1080/01430750.2015.1092471

Singh AK, Samsher (2020) Material conscious energy matrix and enviro-economic analysis of passive ETC solar still. Mater Today Proc 38:1–5. https://doi.org/10.1016/j.matpr.2020.05.117

Singh AK, Singh DB, Mallick A, Kumar N (2018) Energy matrices and efficiency analyses of solar distiller units: a review. Sol Energy 173:53–75. https://doi.org/10.1016/j.solener.2018.07.020

Subramanian RS, Kumaresan G, Ajith R et al (2021) Performance analysis of modified solar still integrated with flat plate collector. Mater Today Proc 45:1382–1387. https://doi.org/10.1016/j.matpr.2020.06.409

Tiwari S, Tiwari GN (2016) Thermal analysis of photovoltaic-thermal (PVT) single slope roof integrated greenhouse solar dryer. Sol Energy 138:128–136. https://doi.org/10.1016/j.solener.2016.09.014

Wang Z, Duan Z, Zhao X, Chen M (2012) Dynamic performance of a façade-based solar loop heat pipe water heating system. Sol Energy 86:1632–1647. https://doi.org/10.1016/j.solener.2012.02.031

Yadav Y (1991) Analytical performance of a solar still integrated with a flat plate solar collector: thermosiphon mode. Energy Convers Manag 31:255–263

Zheng Y, Hatzell KB (2020) Technoeconomic analysis of solar thermal desalination. Desalination 474:114168. https://doi.org/10.1016/j.desal.2019.114168